Wat. Res. Vol. 28, No. 1, pp. 107–118, 1994
Printed in Great Britain.

0043-1354/94 $6.00 + 0.00

SUBMICRON PARTICLES IN THE RHINE RIVER—II. COMPARISON OF FIELD OBSERVATIONS AND MODEL PREDICTIONS

MEREDITH E. NEWMAN, MONTSERRAT FILELLA, YUWEI CHEN, JEAN-CLAUDE NÈGRE, DIDIER PERRET* and JACQUES BUFFLE†

Department of Analytical, Inorganic and Applied Chemistry, University of Geneva, 30 Quai Ernest Ansermet, CH-1211 Geneva 4, Switzerland

(First received July 1992; accepted in revised form April 1993)

Abstract—The particle size distribution in the Rhine River near Basle (Switzerland) was measured for a period of over 1 year. Peaks in the measured size distributions were consistently observed in the ranges of 100–200, 300–700 nm and 1–3 μm. The size distributions observed did not vary greatly with time or flow rate. Predictions of a classical coagulation/sedimentation model agreed well with these field observations. This agreement between model predictions and field measurements indicated that the unknown (and probably dynamic) "initial" particle distribution may have been quickly transformed, either in the river or in the interstitial soil solution, through coagulation and sedimentation into the characteristic and relatively stable shape experimentally observed.

Key words—aquatic colloids, river, submicron particles

INTRODUCTION

The importance of submicron particles (subsequently called colloidal particles or colloids) to the distribution of pollutants in natural aquatic systems has recently been recognized (Baker *et al.*, 1986; Morel and Gschwend, 1987; Sigleo and Means, 1990). Colloidal particles may sorb significant quantities of both organic and inorganic pollutants due to their large surface areas relative to their mass. The relative surface area available for sorption is, of course, a function of colloidal size. The fate of colloidal particles is a function of their size distribution, morphology and composition, as well as the chemistry and flow-patterns of the surrounding water body. Thus the particle size distribution may influence both the mass of a pollutant which will sorb to colloidal particles and whether the particles and sorbed pollutant will remain in suspension or coagulate and sediment to a river or lake bed.

In spite of its importance, little information currently exists on the size distribution and behavior of colloidal particles in surface waters (Laxen and Chandler, 1983; Nomizu *et al.*, 1987; Salbu *et al.*, 1987; Orlandini *et al.*, 1990; Salbu and Bjørnstad, 1990). This is partially due to the difficulty in determining submicron particle size distributions. We have studied the particle size distribution in the Rhine River near Basle, Switzerland for a period of over 1 year (Perret *et al.*, 1994). In this article we evaluate the relationship between the observed particle size distributions, and the season and the flow-rate of the river. We also compare the observed particle size distributions to those predicted by a classical coagulation/sedimentation model in order to ascertain whether currently available coagulation/sedimentation theory can help to explain the particle size distributions in the Rhine River, especially in the submicron domain. The assumptions of such classical coagulation/sedimentation models are not directly applicable to rivers. However, our present purpose is not to model colloid transport in the river, but rather to semi-quantitatively explore the role of coagulation and sedimentation in controlling the size distribution of submicron particles observed in the river.

METHODS

Experimental Methodology

Water samples were collected from the Rhine River at Birsfelden (Basle, Switzerland) approximately bimonthly. Samples were collected 1 m below surface level using a high speed pump. The sampling procedure and site have been described in detail by Perret *et al.* (1994). Samples were fractionated by sedimentation followed by cascade centrifugation and filtration as described by Perret *et al.* (1994). The sedimentation and first and second centrifugation steps were carried out in the field immediately after sample collection in order to reduce the possibility of coagulation prior to analysis.

*Present address: Institute of Inorganic and Analytical Chemistry, University of Lausanne, 3 Place du Château, CH-1005 Lausanne, Switzerland.
†Author to whom all correspondence should be addressed.

The particle size distribution was measured using a Malvern, Zeta Sizer III, photon correlation spectrophotometer (PCS), as previously described (Newman and Buffle, 1994; Perret *et al.*, 1994). Samples were also examined by transmission electron microscopy (TEM) (Zeiss EM109) and the composition of the various size fractions was determined by inductively coupled plasma–atomic emission spectrometry (ICP–AES) (Perkin–Elmer, Plasma 1000) (Perret *et al.*, 1994) and total organic carbon (TOC) analysis (Dohrman, DC80).

PCS analyses reported here were carried out at a minimum of three scattering angles in order to check for masking of small particles by the presence of larger more efficient scatterers, and to verify that all particles, present in sufficient numbers to be identified, were found (Schurtenbeger and Newman, 1993). The mean and standard deviations reported here are based on a minimum of three, and frequently as many as 15, replicates. These replicates include analyses made at varying scattering angles. Therefore variation due to the presence of nonspherical, irregularly-shaped particles is included in these standard deviation values.

The total mass of the raw sample and of a sedimented sample was measured by filtration and gravimetry. The length of the sedimentation step was chosen to allow removal of larger, more dense particles (Perret *et al.*, 1994). Based on Stokes' law it was estimated that particles greater than 3 μm in diameter with densities greater than 1.5 g cm^{-3} (Jerlov, 1976; CRC, 1989) were removed during the sedimentation step. The difference in the mass measured for a raw and sedimented sample was then taken to represent the percentage of the total mass greater than 3000 nm in diameter.

Mie analysis (Ford, 1983) was used to convert the intensity weighted size distributions obtained by PCS to volume (mass) weighted distributions and subsequently to the percent of total mass in various size classes (Bott, 1988; Van der Meeren *et al.*, 1988; Newman and Buffle, 1994). Size classes were set at <200 nm, 200–700 nm, 700 nm–1 μm, 1–3 μm and >3 μm based on the size ranges most frequently observed for peaks in the size distributions.

A complete size distribution could not be obtained from a single, unfractionated, sample due to the broad range of sizes present in the Rhine samples, and the limited resolution possible with PCS. Therefore, a combination of the particle mass removed during the sedimentation step, as described previously, and mass weighted size distributions obtained both for the sedimented sample and the supernatant from a 5 h centrifugation (3700 ***g***) [second centrifugation step; see Perret *et al.* (1994), Fig. 1 for the complete fractionation scheme] was used to estimate a composite distribution. The percentages of particle mass within the two size classes, 700 nm–1 μm and 1–3 μm, and the percentage of particle mass <700 nm were based on the results for the sedimented samples. The percentages of particle mass between 200 and 700 and <200 nm were then estimated by multiplying the percentages measured in the supernatant of the second centrifugation step (5 h at 3700 ***g***) by the percentage of particles <700 nm estimated from the sedimented samples (see Fig. 1). The supernatant of the second centrifugation step (5 h at 3700 ***g***) was used preferentially to that of the first centrifugation step (0.5 h at 520 ***g***) because separation of particles smaller and larger than 700 nm has been found to be more efficient in the latter centrifugation.

The percent error associated with mass weighted size distribution measurements was estimated to be approx. 10–15% as discussed in Newman and Buffle (1994). This error was propagated in the subsequent calculations. Based on the standard deviations between replicates for the total mass and sedimented mass measurements and a generous allowance for the assumptions (such as estimation of particle density), the total error associated with estimates of the percentage of total mass in the various size classes is approx. 35–45%.

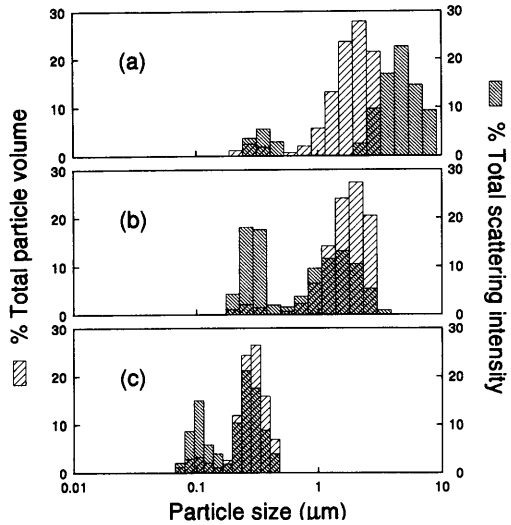

Fig. 1. Particle size distributions measured by PCS for a sample collected from the Rhine River on 6 November 1990. (a) Raw sample, (b) after a 2 h sedimentation, (c) after centrifugation for 1.5 h at 3700 ***g***. Particles in the raw sample were larger than the upper limit of PCS and frequently sedimented between replicate analyses.

Modeling Methodology

Model description

Basic coagulation theory for hydrophobic colloids, which is largely based on the seminal work of Von Smoluchowski (1918), has been presented in detail elsewhere (Friedlander, 1977; O'Melia, 1980, 1987; Stumm and Morgan, 1981; Hirtzel and Rajagopalan, 1985). Combining the physical processes controlling colloid collision, as presented in Table 1, the collision efficiency, and Stokes' law for gravitational sedimentation yields the dynamic equation that describes the transport of particles in aquatic systems.

The dynamic equation for the particle size distribution (discrete form) is given by

$$\frac{dn_k}{dt} = \frac{1}{2}\sum_{(vi+vj=vk)} \alpha(i,j)\cdot\beta(i,j)\cdot n_i\cdot n_j - n_k\cdot\sum_{(i=1,\infty)}\alpha(i,k)\cdot\beta(i,k)\cdot n_i - (w_k/z)\,n_k \quad (1)$$

where n_i, n_j, n_k denote the number concentration of particles of sizes i, j, k (L^{-3}); $\alpha(i,j)$ is the collision efficiency, which includes the chemical nature of the particles and the solution (dimensionless); $\beta(i,j)$ is a collision frequency function, which depends upon the hydrodynamic mode of interparticle approach (L^{-3}T^{-1}) (see Table 1 for the functional relationships for the three particle collision mechanisms considered); w_k is the settling velocity of particles of size k assumed by Stokes' law (LT^{-1}), and z is the depth (L).

The left-hand side of equation (1) describes the rate at which the number concentration of particles of size k changes with time (L^{-3}T^{-1}). The first term on the right-hand side of equation (1) expresses the formation rate of particles of size k from smaller particles (i,j) having a total volume v_k. The second term describes the loss of particles of size k by formation of larger aggregates. The third term describes the loss of size k particles from suspension by settling.

Table 1. Functional relationships for the three particle collision mechanisms considered and for Stokes settling rate

Brownian motion (thermal effects) $\beta(i,j) = K_b[(1/v_i)^{1/3} + (1/v_j)^{1/3}](v_i^{1/3} + v_j^{1/3})$ $K_b = 2kT/3\,\mu$	$(L^3\,T^{-1})$
Fluid shear (flow effects) $\beta(i,j) = K_{sh}(v_i^{1/3} + v_j^{1/3})^3$ $K_{sh} = G/\pi$	(T^{-1})
Differential settling (gravity effects) $\beta(i,j) = K_{ds}(v_i^{1/3} + v_j^{1/3})^3\lvert v_i^{1/3} - v_j^{1/3}\rvert$ $K_{ds} = (6/\pi)^{1/3}(g/12\,\mu)(\rho_p - \rho)$	$(L^{-1}\,T^{-1})$
Stokes settling $w_i = S \cdot v_i^{2/3}$ $S = (1/6\,\pi^2)^{1/3}(g/3\,\mu)(\rho_p - \rho)$	$(L^{-1}\,T^{-1})$

v_i, v_j = particle volume; k = Boltzmann's constant; T = absolute temperature; μ = water viscosity; G = mean velocity gradient; g = gravitational acceleration; ρ_p = particle density; ρ = water density.

No general analytical solution exists for the dynamic equation coupling coagulation with sedimentation: it must be solved either using simplified analytical solutions or numerically. In the present work the particle size distribution has been expressed as a finite number of size intervals, and a set of differential equations of the form of equation (1) have been integrated numerically over time (Lawler *et al.*, 1980; O'Melia and Bowman, 1984). For details concerning selection of size intervals and criteria for assigning newly formed particles to standard particle size classes, see Lawler *et al.* (1980). The model has previously been applied to lakes by O'Melia and co-workers (O'Melia and Bowman, 1984; Ali *et al.*, 1985; O'Melia *et al.*, 1985; Weilenmann *et al.*, 1989).

Model limitations

In the development of the model the following assumptions are made: (i) colloids are hydrophobic, (ii) particles are of identical nature (chemically homogeneous), (iii) particles before and after each aggregation are rigid spheres, (iv) volume of solid particles is conserved during agglomeration, (v) particles approach one another on rectilinear paths, the path of one particle not being affected by the presence of another, (vi) collision functions for Brownian motion, fluid shear and differential settling are assumed to be additive, (vii) only binary particle encounters are assumed to occur, (viii) breakup or dissociation of aggregates due to fluid shear or other processes are not included and (ix) the river is considered as an idealized settling basin: horizontal transport (the rate of horizontal flow and the physical shape of the river) has not been taken into account. As explained in the Introduction these assumptions are not directly applicable to a river system. However, keeping this in mind, and in the absence of more appropriate models, predictions of this existing model are helpful for qualitatively interpreting the behavior of river colloids.

Table 2. River properties used in the model calculations

Property	Value
Mean half depth (m)	2.5
Temperature (°C)	15
Water viscosity ($g\,cm^{-1}\,s^{-1}$)	1.146×10^{-2}
Water density ($g\,cm^{-3}$)	0.999
Velocity gradient, G (s^{-1})	10
Coagulation efficiency, α	0.05
Particle density ($g\,cm^{-3}$)	1.5
Initial particle distribution	Varied
Initial particle concentration	Varied

Values used in the model simulations

The values of the parameters used in the model simulations are indicated in Table 2. Some more important parameters will be discussed briefly below. Properties such as mean depth and water temperature were directly determined by the values measured for the Rhine River. Certain other parameters which could not be easily measured have been estimated and, in some cases, their influence has been tested by varying their values in the modeling simulations. The estimated parameters are the mean velocity gradient, the particle density and the coagulation efficiency.

Mean velocity gradient. The mean velocity gradient, G, reflects the rate at which particles contact due to velocity gradients within the flowing fluid. In the present work a mean value of $10\,s^{-1}$ (Stumm, 1977; Stumm and Morgan, 1981) has been selected as characteristic of Rhine River conditions.

Particle density. For model calculations some assumptions about particle density were necessary. Although it is clear that in natural systems a wide range of density values exists (a direct consequence of the diversity of particle types present), particle density was assumed to be constant over the entire size distribution and for all particle types present. The density value assumed in the model was $1.5\,g\,cm^{-3}$ which has been shown to be representative of observations in natural waters (Jerlov, 1976; CRC, 1989; Weilenmann *et al.*, 1989).

Coagulation efficiency. Colloid stabilities can be quantitatively compared using the stability ratio, α. α is a semi-empirical dimensionless parameter which is equivalent to the fraction of interparticle collisions that result in aggregation. For a perfectly stable suspension (no successful collisions), $\alpha = 0$. For a completely destabilized suspension (all collisions produce aggregation), $\alpha = 1$.

Estimates of α have been calculated in several laboratories using various particles and solutions (Swift and Friedlander, 1964; Birkner and Morgan, 1968; Hahn and Stumm, 1968; Edzwald *et al.*, 1974; Tipping and Higgins, 1982; Kebler *et al.*, 1989). Particle stability ratios measured experimentally for fresh surface waters range over two orders of magnitude, from about 0.001 to more than 0.1 (Gibbs, 1983; Ali *et al.*, 1984; Weilenmann *et al.*, 1989). Solution chemistry (including pH, ionic strength and the specific cations and anions in solution) as well as surface properties of the particles control the colloidal stability of natural particles in aquatic systems: in particular calcium may destabilize colloids (α increases) while dissolved organic matter may stabilize them (α decreases).

An α value of 0.05 was used in these simulations. This value falls within the values found in the literature for water with calcium concentrations and total organic carbon content similar to those of the Rhine River (dissolved organic carbon = $1.5\,mg\,dm^{-3}$, calcium concentration = $2\,mmol\,dm^{-3}$).

EXPERIMENTAL RESULTS

Size distribution

The range of particle sizes observed on a single sampling date, and over the course of the year, was continuous from approx. 50 nm to well above the upper limit of PCS, approx. 3 μm. However, peaks in the size distribution were generally observed for particles in the ranges of 100–200 nm, 300–700 nm and 1–3 μm (see Figs 1 and 2). The size distributions observed in the Rhine River lie within the broad range of values observed in other rivers (see Table 3). Note, however, that very few detailed size distributions have been reported in the literature. Most of

these data have been obtained by chemical analysis or gravimetry of filtered fractions.

The sensitivity and subsequently the detection limit of PCS rapidly decrease as the particle size decreases below approx. 25 nm (Newman and Buffle, 1994). Therefore, based on PCS results, it was not possible to say whether particles smaller than 50 nm were absent in the river samples or present in concentrations below the detection limit. TEM micrographs indicated that colloids smaller than 50 nm were present, however they were most often either coagulated with other small colloids or enmeshed in large organic matrices, and may not have been present as independent particles (Filella *et al.*, 1993; Perret *et al.*, 1994). Perret *et al.* (1994) showed that special sample preparation and imaging techniques must be used to successfully image organic structures by TEM. Therefore organic–inorganic associations may often be overlooked by TEM. Scanning electron microscopy (SEM) images of colloidal particles from the Mississippi River also indicated that the majority of the particles present were coagulated to some degree (Leenheer *et al.*, 1988; Rees, 1990; Rees and Ranville, 1990).

Although there was variation in the mean values for peaks in the size distribution over time, this variation was not obviously related to season. The presence of three peaks and the approximate size range of the peaks also appeared to be relatively constant over time (see Fig. 2). A lack of seasonal variation in colloidal particle size was also observed by Ford and Lock (1985) for two Welsh rivers.

The colloidal size distribution did not appear to be greatly influenced by changes in river flow-rate. The flow-rate varied from a background rate ranging from 630 $m^3 s^{-1}$ (September 1990) to 1235 $m^3 s^{-1}$ (November 1990) to a flood condition during which the flow-rate could not be measured (June 1991).

Mass fractions in the various size classes

The mass fractions estimated by weighing and PCS are given in Table 4 and Fig. 3. Although the mass of fractions larger than a few hundreds of nanometers increased significantly during flood periods (June 1991), such was not the case for colloids $\leqslant 200$ nm. These observations were confirmed by ICP analysis (see below). Figure 3(a) also suggests that the proportions of mass fractions < 1000 nm were most often between 0 and 10%, while the proportions of fractions > 1000 nm were more variable but were not obviously related to flood events.

Although ICP analyses of raw and sedimented samples might have underestimated the true values for the reasons given in Perret *et al.* (1994), it was

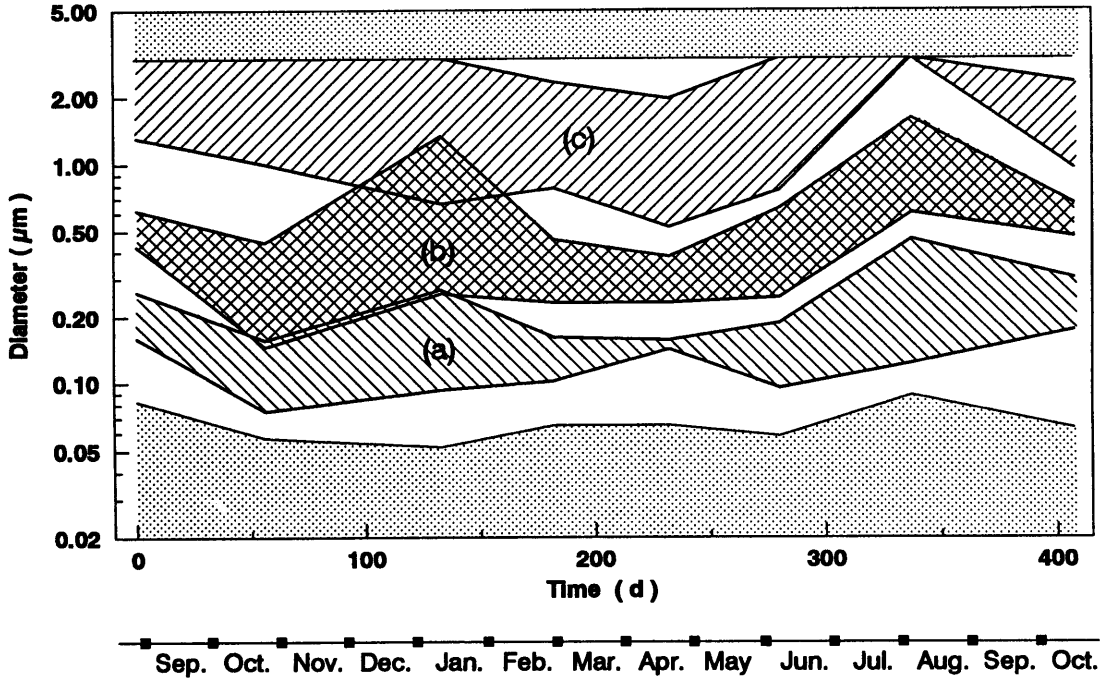

Fig. 2. Range of mean values for peaks in the particle size distribution measured by PCS from September 1990 through October 1991 (see "Experimental Methodology" for the significance of mean values). The peak means fall primarily in three domains: (a) 100–200 nm; (b) 300–700 nm; (c) 1000–3000 nm. The smallest size detected by PCS is also indicated. The maximum size measurable by PCS is approx. 3000 nm (depending on particle density).

Table 3. Colloidal particles observed in river samples

River sampled	Techniques used*	Sizes observed†	Peaks in size distribution	Comments	Reference
Rhine, Holland	filtration	5 nm–60 μm	3–12 μm‡	colloids <400 nm made up 5–13% of the total mass	Van de Meent *et al.* (1983)
Mississippi, Illinois, Missouri, Ohio, White, Arkansas, U.S.A.	sedimentation, filtration, photosedimentation¶, PCS, SEM		260–440 nm§ 310–360 nm 400–480 nm 280 nm 300–320 nm 270–280 nm	relationship observed between colloid concentration and river flow-rate colloids <3 μm made up 51% of the total mass	Leenheer *et al.* (1988) Rees (1990) Rees and Ranville (1990)
Chuckwa Creek, U.S.A.	sedimentation, sieving, PCS	290 nm–1.26 μm	480–730 nm		Gallegos and Manzel (1987)
Shonaigawa, Japan	centrifugation, TEM	10 nm–100 nm 100 nm–1 μm			Nomizu *et al.* (1987) Nomizu *et al.* (1988)
St Lawrence, Canada	filtration, centrifugation	300 nm–>8 μm		the greatest mass of particles in classes >8 μm or 0.4–8 μm peaks related to seasonal variation in river flow-rate	Comba and Kaiser (1990)
Glatt, Switzerland	filtration	2–450 nm		colloid concentration constant at normal flow but elevated during floods	Waber *et al.* (1990)
Price, Green, Colorado, U.S.A.	sedimentation-FFF‖		100, 200 nm**		Karaiskakis *et al.* (1982)
Yarra, Australia	sedimentation-FFF‖	100–500 nm	220 nm		Becket *et al.* (1988)
Mississippi, U.S.A.	filtration	<1000 MW–>100,000 MW††			Hoffmann *et al.* (1981)
Clywedog, Aber, Wales	filtration	<1000 MW–0.7 μm††		no seasonal variation in sizes observed	Ford and Lock (1985)
Boreal high order streams,	filtration	100,000 MW–0.7 μm†† 100,000 MW–300,000 MW††			Lock and Ford (1986)
Boreal 1st order streams, Canada	filtration	<15 nm–1 μm††			Hiraide *et al.* (1989)

*The size distribution obtained is a function of the weighting (mass, volume, number, or light scattering intensity) method employed in the analytical technique used. The distributions produced by these various methods are not directly comparable without first correcting to a common weighting method.
†The sizes observed were frequently limited by the method of analysis and/or the size range of interest to the investigator.
‡These values represent the size ranges in which the greatest mass of particles was observed by gravimetry of filtered samples.
§These values represent peak means estimated by PCS or photosedimentation.
¶Photosedimentation analysis is a technique which utilizes the change in optical density of a suspension of colloidal material in a centrifugal field.
‖Sedimentation field flow fractionation (FFF) utilizes a perpendicular centrifugal force to fractionate particle suspensions flowing through a thin channel.
**Peak positions depend on field applied.
††Colloidal organic matter.

Table 4. Particle mass observed in each size class of the Rhine River samples

Date*	Size class (nm)	Mass (mg dm^{-3})	Percent of total mass
22/1/91	>3000	2.4	38.8
	1000–3000	2.8	46.6
	700–1000	0.2	2.9
	200–700	0.5	9.3
	<200	0.2	2.4
	Total	6.1	100
12/3/91	>3000	1.8	28.5
	1000–3000	3.7	57.2
	700–1000	0.2	3.2
	200–700	0.7	10.1
	<200	0.1	1.1
	Total	6.5	100
30/4/91	>3000	2.9	54.0
	1000–3000	0.9	16.6
	700–1000	0.6	11.5
	200–700	0.9	17.3
	<200	0.1	0.6
	Total	5.4	100
17/6/91	>3000	637.6	91.0
	1000–3000	16.1	2.3
	700–1000	1.4	0.2
	200–700	45.5	6.5
	<200	0	0
	Total	700.6	100
13/8/91	>3000	8.8	81.7
	1000–3000	0.7	6.7
	700–1000	0.3	2.8
	200–700	0.8	7.1
	<200	0.2	1.7
	Total	10.8	100
22/10/91	>3000	4.2	60.0
	1000–3000	2.0	27.7
	700–1000	0.1	1.8
	200–700	0.5	6.9
	<200	0.2	3.0
	Total	7.1	100

*Samples were collected on six dates. Duplicate samples were collected on each sampling date. Each duplicate was then fractionated and multiple analysis (3–15) were performed on each fraction.

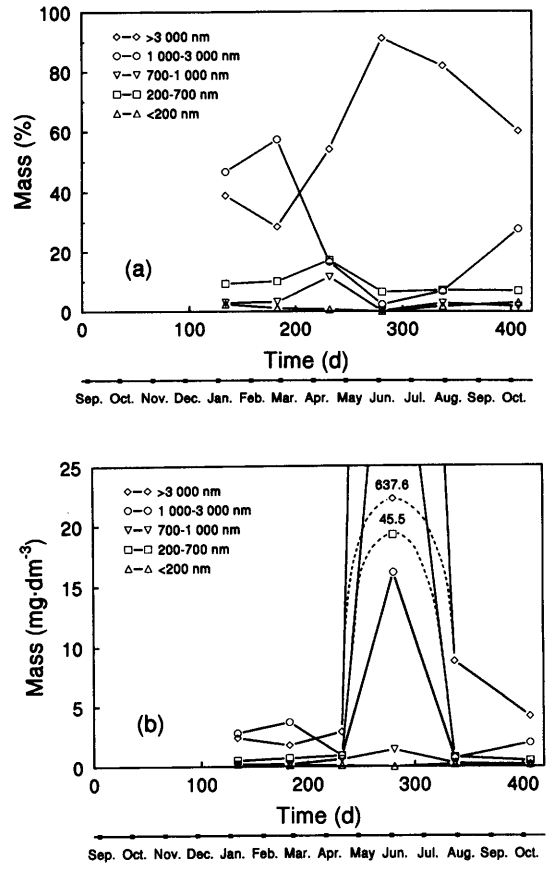

Fig. 3. (a) Percentage of mass concentration and (b) total mass concentration in the various size classes in the Rhine River from September 1990 through October 1991.

possible to observe the seasonal evolution of the elemental concentrations in the various size fractions. The results [Fig. 4(a)–(c)] indicated that the composition of the various colloidal size classes varied little with time or flow-rate. As mentioned above, ICP analyses also showed the concentration of larger particles to be strongly influenced by river flow-rate while the concentration of smaller particles (<200 nm) was much less affected [Fig. 4(a)–(c)].

A similar trend was observed for the organic matter content as measured by TOC. TOC could not be measured in centrifuged fractions, for the reasons given in Perret *et al.* (1994), but the time evolution of TOC in raw water, sedimented samples and filtrates of 0.8 and 0.05 μm pore size membranes are given in Fig. 4(d). In all "normal" flow-rate situations, the organic matter content of raw water was primarily composed of molecules smaller than 0.05 μm. This agrees with the generalization that in aquatic systems containing primarily pedogenic organic matter, the "particulate" organic carbon (>0.45 μm) represents $\leqslant$10% of the TOC (Buffle, 1988). On the other hand, during the flood event of June the proportion of organic matter >0.8 μm increased significantly [Fig. 4(d)], as did inorganic elements [Fig. 4(a)–(c)]. Zumstein and Buffle (1989) also observed the "particulate" pedogenic organic matter content of rivers to be correlated to storm events.

The cause of the size dependent effect of river flow-rate on mass loading is not known. However, an intuitive explanation is that the increased river velocity during the flood maintained large particles in suspension which would have sedimented at normal velocities. Submicron colloids do not require increased velocities to remain in solution since their sedimentation rate is extremely slow even during quiescent conditions.

Similar observations of increases in the mass concentration of larger particles during periods of high flow have been made in the Glatt River in Switzerland (Waber *et al.*, 1990) and several rivers in the U.S.A. (Leenheer *et al.*, 1988; Rees, 1990; Rees and Ranville, 1990). Lock and Ford (1986) observed that the mass concentration of larger particles in several Canadian rivers decreased during periods of extremely low flow at the end of summer and after the beginning of winter freezing.

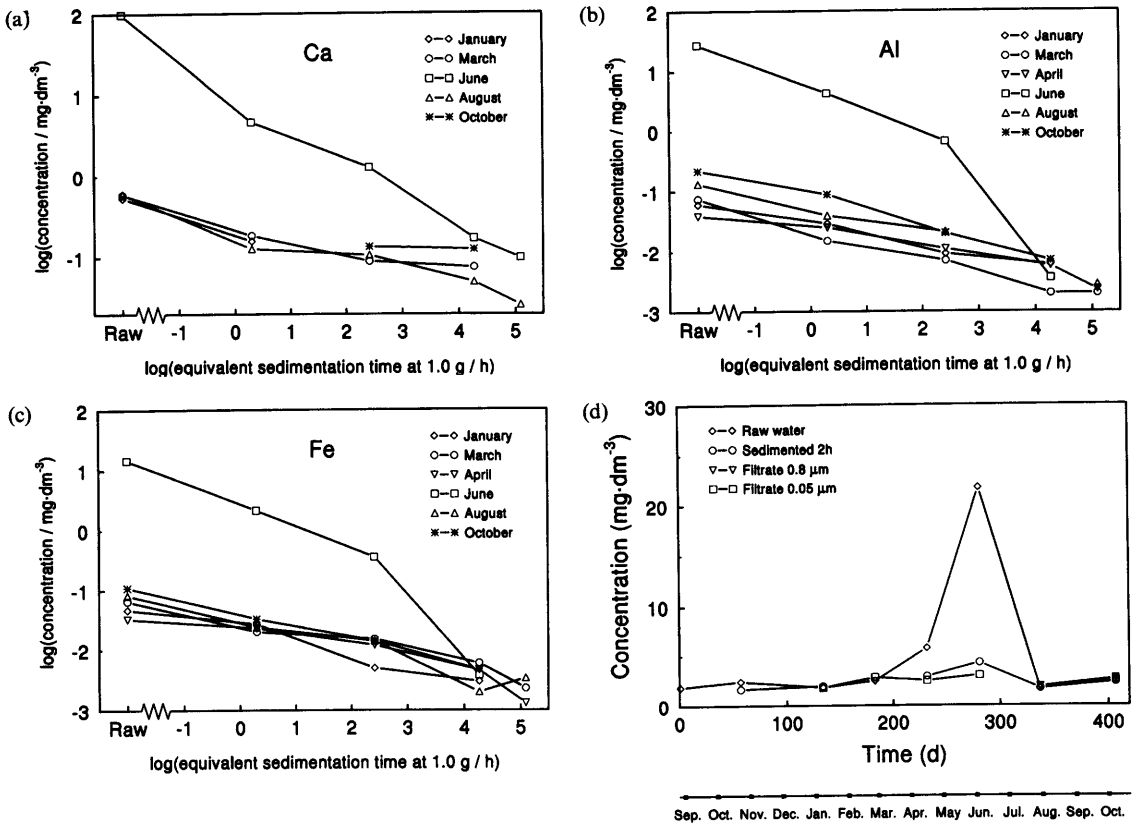

Fig. 4. (a)–(c) The mass concentration of Ca, Al and Fe measured by ICP for each sampling date. The abscissa gives the equivalent sedimentation time at 1 *g* for the raw sample, sedimented sample, and first, second and third centrifuged fraction [the position of the raw sample is arbitrary; see Perret *et al.*, 1994), Table 1 for the estimated maximum particle size in each fraction]. The metal concentrations observed were similar for all sampling dates except during the flood event in June. During June the samples containing large particles (raw, sedimented, supernatant of first centrifugation), exhibited significantly higher metal concentrations. The supernatant of the second centrifugation, which contained smaller particles, varied less. (d) Time evolution of TOC in the raw water, sedimented samples and filtrates of 0.8 and 0.05 μm pore size membranes.

The mass concentration and the percentage of total mass in each size class for each sampling date are listed in Table 4. The average percentage of the total particle mass in each size class over the entire sampling period was:

Size (nm)	Percent of total mass (mean $\pm$ 1 σ)
>3000	59.1 $\pm$ 24.1
1000–3000	26.2 $\pm$ 22.0
700–1000	3.7 $\pm$ 3.9
200–700	9.5 $\pm$ 4.0
<200	1.5 $\pm$ 1.1

These values agree with values measured using mass fractionation by filtration in the Rhine River in Holland (Van de Meent *et al.*, 1987) and several major rivers in the U.S.A. (Leenheer *et al.*, 1988; Rees, 1990; Rees and Ranville, 1990) (Table 3).

Results of modeling simulations

The effect of varying initial mass particle concentration, initial particle size distribution, and time on the calculated size distributions was analyzed because the total mass particle concentration and the initial size distribution were either unknown or varied with time and location. Previous simulations demonstrated that model predictions were less sensitive to changes in G or α than to particle concentration or initial particle size distribution (Filella and Buffle, 1993). Given the wide range of particle sizes considered in the numerical solution, the use of a logarithmic division of particle sizes was necessary.

Results are presented as discrete plots of particle volume, $dV/d(\log d_p)$, versus $\log d_p$ (d_p = particle diameter). This representation was chosen because it has the advantage that the total volume concentration between any two sizes is equal to the area under the curve between those sizes (Stumm and Morgan, 1981).

Figure 5(a), (b) and (c) shows the size distribution evolution with time for three initially monodisperse suspensions having the same initial mass concentration (1 mg dm^{-3}) but different sizes: (i) 10 nm particles [Fig. 5(a)]; (ii) 200 nm particles [Fig. 5(b)]; (iii) 4 μm particles [Fig. 5(c)]. Similar evolutions for the same initially monodisperse suspensions, but for initial mass particle concentrations closer to those measured in the river for each particle class, were also calculated: (i) 0.01 mg dm^{-3} for 10 nm particles (0.1% of the total mass concentration in the river, see Table 4) [Fig. 6(a)]; (ii) 0.2 mg dm^{-3} for 200 nm particles (2% of the total mass concentration) [Fig. 6(b)]; (iii) 6 mg dm^{-3} for 4 μm particles (60% of the total mass concentration) [Fig. 6(c)].

From Figs 5 and 6 it is evident that particles smaller than 200 nm were predicted to coagulate rapidly even at quite low concentrations: all 10 nm particles disappeared in less than 2 h forming more stable agglomerates of 100–300 nm. Particles of 200 nm coagulated slowly to give agglomerates hardly larger than the initial 200 nm particles. Four micrometer particles disappeared fairly rapidly by sedimentation.

From these figures a dependence of the size distribution evolution on the initial mass concentration and on time may be deduced. To gain further insight into this dependence specific simulations were performed. Figure 7(a) shows the evolution with time (up to 8 days) for an initially monodisperse solution (200 nm) with an initial mass concentration close to that observed in the river (0.2 mg dm^{-3}). The same results but represented as the evolution of the mean size with time are depicted in Fig. 7(b). These figures confirm that particles of this size range undergo a slow coagulation process.

Figure 8(a) shows the distributions obtained for the same initially monodisperse suspension (200 nm) after 2 days when the initial mass concentration varies over three orders of magnitude (from 0.01 to 10 mg dm^{-3}). Figure 8(b) shows the change in the mean size with time under the same conditions. The effect of increasing particle concentration demonstrated by these simulations might explain the fact that the mass concentration of particles smaller than 200 nm was estimated to be zero for the sample taken during the flood when the total mass particle concentration was nearly 700 mg dm^{-3}.

The size distribution evolution with time for the case of an initially tridisperse system: uniform concentration (1 mg dm^{-3} each) of 10 nm, 200 nm and 4 μm particles is shown in Fig. 9. The results obtained confirm the previous observations: the small particles disappear rapidly while a stable peak appears at 100–300 nm. Larger particles are removed by sedimentation.

Similar behavior can be observed in Fig. 10 where the evolution of an initially continuous particle size

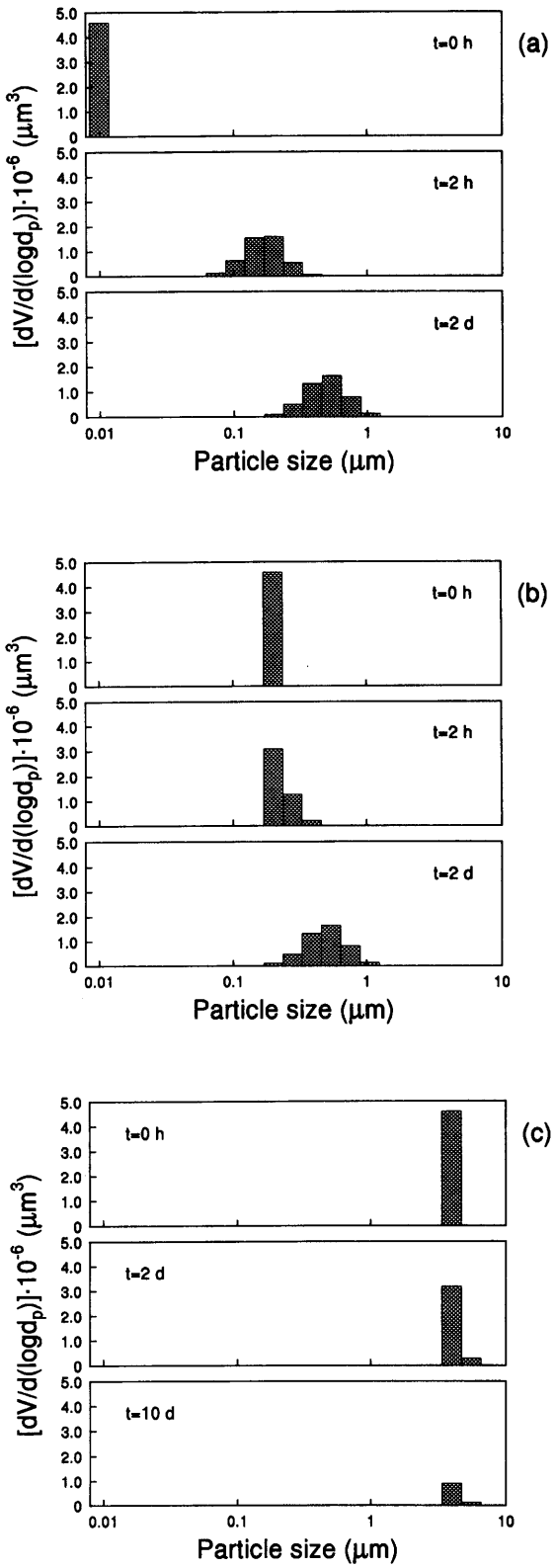

Fig. 5. Simulation results for (a) an initially monodisperse 10 nm particle size distribution; (b) an initially monodisperse 200 nm particle size distribution; (c) an initially monodisperse 4 μm particle size distribution. Initial particle concentration = 1.0 mg dm^{-3} in all cases. Values of other parameters as in Table 2.

distribution (power law distribution with $\beta = 4$)* ranging from 1 nm to 100 μm is shown.

DISCUSSION

As previously mentioned, size distributions observed in the Rhine River were relatively constant with time and appeared to be little influenced by changes in season or river flow-rate. Although, as previously discussed, the coagulation/sedimentation model used required several simplifying assumptions, size distributions predicted by the model agreed reasonably well with the distributions observed in the river.

This agreement between model predictions and field observations may have resulted from either one or both of the following two processes: (i) the observed particle size distribution, or at least its lower range, resulted from coagulation processes occurring within the interstitial soil solution prior to entering the river; (ii) the unknown (and probably dynamic) "initial" particle size distribution leached from the soil into the river was rapidly transformed through coagulation and sedimentation into the characteristic and relatively stable shape experimentally observed, with depletion in both small and large particles.

Well separated colloidal particles smaller than 50 nm were observed by medium resolution TEM (Perret *et al.*, 1994). One explanation for this discrepancy between classical model predictions and these TEM observations is that coagulation of very small colloids may not occur only with other hydrophobic particles but also with hydrophilic organic macromolecules and matrices. Such colloid–organic matrix associations were frequently observed by high contrast, high resolution TEM in the Rhine River samples (Perret *et al.*, 1994) and in other surface waters (Filella *et al.*, 1993). Furthermore, since, as mentioned previously, these organic matrices may be difficult to visualize by TEM, some small colloids frequently appear as isolated entities in medium resolution, low contrast TEM images while they

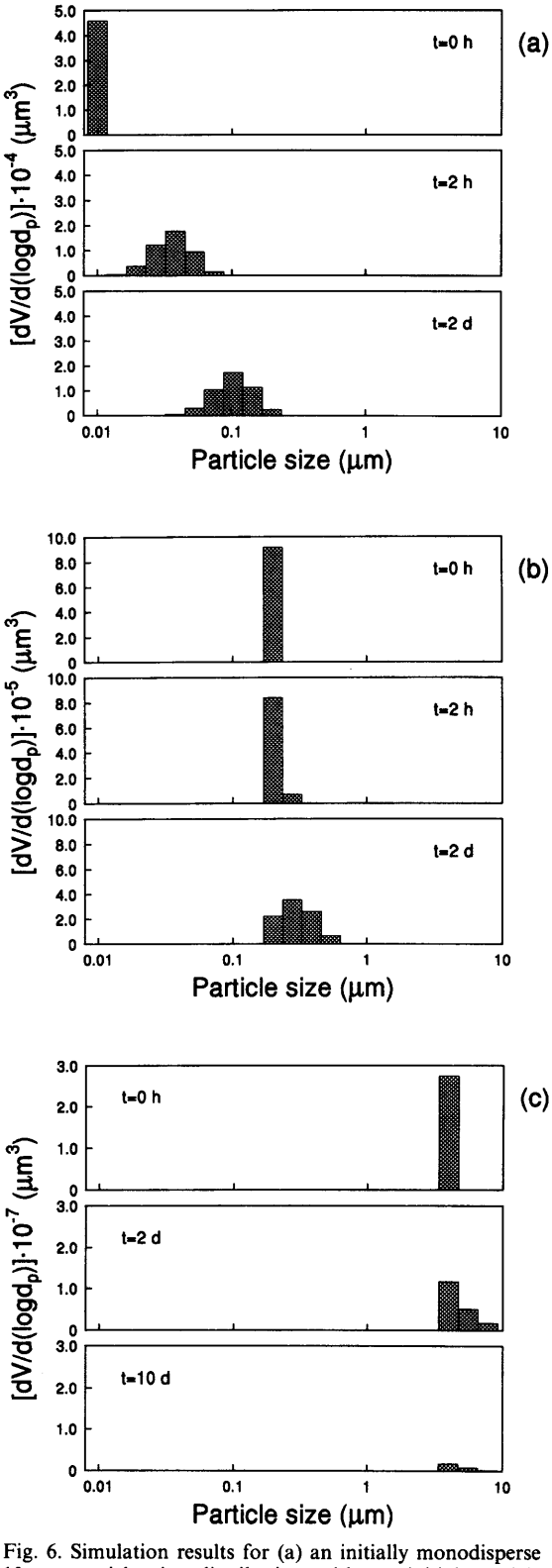

Fig. 6. Simulation results for (a) an initially monodisperse 10 nm particle size distribution with an initial particle concentration = 0.01 mg dm^{-3}; (b) an initially monodisperse 200 nm particle size distribution with an initial particle concentration = 0.2 mg dm^{-3}; (c) an initially monodisperse 4 μm particle size distribution with an initial particle concentration = 6 mg dm^{-3}. Values of other parameters as in Table 2.

*The size distribution function, $n(d_p)$, of a population of coagulating particles is defined by

$$\Delta N = n(d_p) \cdot \Delta d_p$$

where ΔN is the number of particles with a diameter in the size interval Δd_p, per unit volume of fluid. Atmospheric aerosols (Friedlander, 1960) and hydrosols (Lerman *et al.*, 1977; Lerman, 1979; McCave, 1984) are found to exhibit the power law

$$n(d_p) = (\Delta N/\Delta d_p) = C\, d_p^{-\beta}$$

where the exponent β is a constant. For environmental samples, β is found to lie in the range 2.0–5.0 and is near 4.0 in many cases. A particle size distribution following a power law with an exponential coefficient, β, of 4.0 corresponds to an equal distribution of particle volume or mass in every logarithmic size interval.

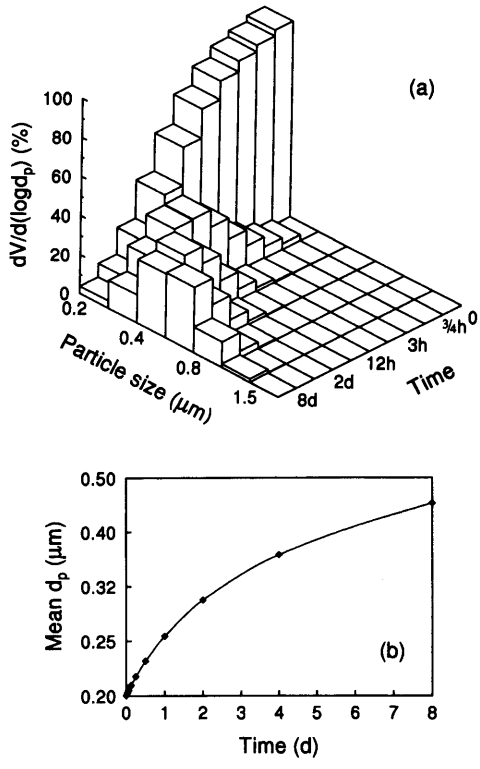

Fig. 7. Simulation results for an initial particle size distribution of 200 nm at different times ranging from 0 to 8 days. Initial mass concentration = 0.2 mg dm^{-3}. (a) Evolution of particle size distribution with time, (b) evolution of weighted mean size with time. Values of other parameters as in Table 2.

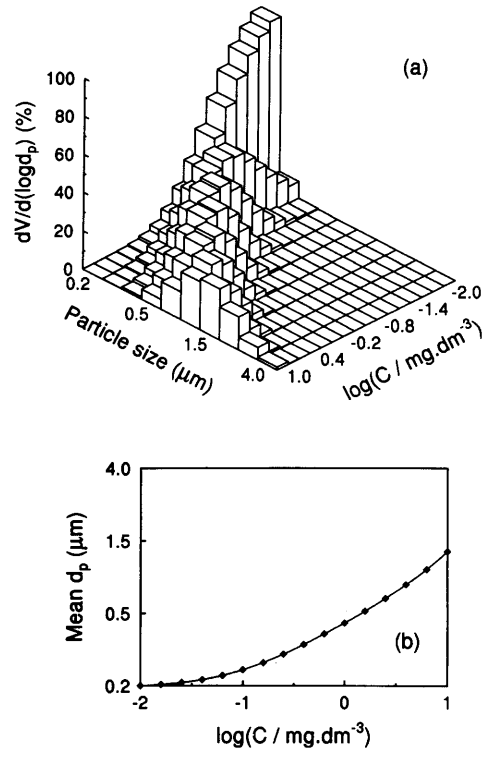

Fig. 8. Simulation results for an initial particle size distribution of 200 nm at 2 days with different initial mass concentrations ranging from 0.01 to 10 mg dm^{-3}. (a) Evolution of particle size distribution with concentration, (b) evolution of weighted mean size with concentration. Values of other parameters as in Table 2.

are, in reality, bound by a very thin filamentous material. Such associations between hydrophobic and hydrophilic colloids are not currently considered by classical coagulation theory, and further study of their formation is necessary.

In any case, both observations and model predictions suggest that particles smaller than 1 μm were controlled by either efficient Brownian coagulation or association with organic matrices either in the interstitial soil solution or in the river, and that large particles entering the river through mechanical soil erosion settled from suspension faster than they were replenished by erosion or coagulation. Although the model predicted particles larger than 3–5 μm to be completely removed by sedimentation, some larger particles probably remained suspended because the hydraulic loading (m s^{-1}) of the river was higher than Stokes' settling velocity. This was confirmed by the observed increase in the mass concentration of particles larger than 1 μm with increasing flow-rate, while the mass concentration of submicron particles was observed to be much less influenced by flow-rate.

In spite of the fact that the mass of particles smaller than 200 nm was observed to be less than 2% of the total particle mass, the number and the total available

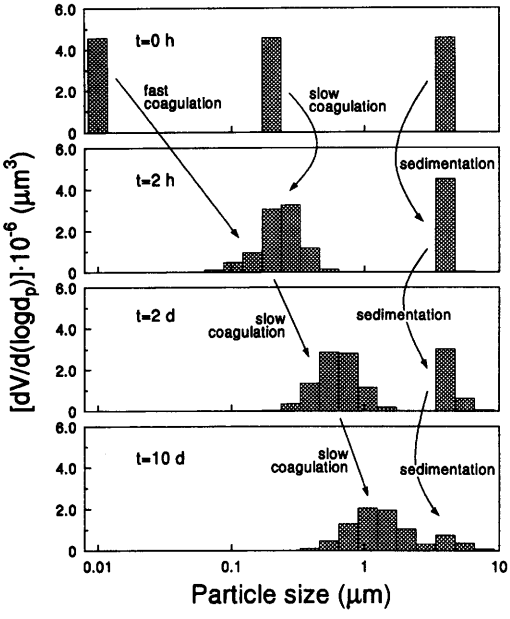

Fig. 9. Simulation results for an initially tridisperse particle size distribution of 10 nm, 200 nm and 4 μm. Initial mass concentration = 1 mg dm^{-3} for each size class (total mass concentration = 3 mg dm^{-3}). Values of other parameters as in Table 2.

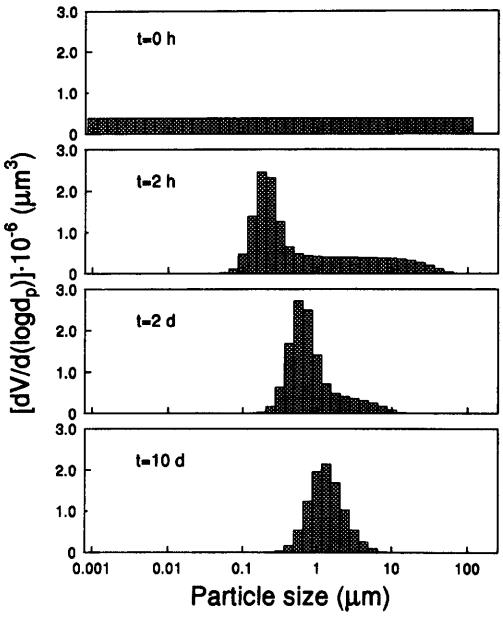

Fig. 10. Simulation results for a continuous initial particle size distribution with $\beta = 4$ and size range from 1 nm to 100 μm. Initial total mass concentration = 3 mg dm^{-3}. Values of other parameters as in Table 2.

surface area of such particles could have remained relatively high compared to that of larger particles. For example, the following three colloidal solutions have the same total surface areas (40 cm^2 dm^{-3}): 0.01 mg dm^{-3} of 10 nm particles, 0.2 mg dm^{-3} of 200 nm particles and 4 mg dm^{-3} of 4 μm particles. Therefore, quite small colloids may play a significant role in the transport of both nutrients and toxic compounds.

CONCLUSION

The results of a comparison of field data with classical coagulation/sedimentation model predictions indicated that the colloidal particle size distribution in the Rhine River was maintained in a relatively steady-state condition by gravitational sedimentation of particles larger than 3–5 μm and by rapid Brownian coagulation and association of particles smaller than approx. 100 nm with organic matrices.

Although particles smaller than 200 nm made up less than 2% of the total particle mass, they contributed significantly to the available colloidal surface area. Because particles of this size are expected to remain in suspension and be transported with the water flow, they may be important to the fate of both organic and inorganic pollutants.

Acknowledgements—The authors gratefully acknowledge the assistance of Dr M. Wiesner (Rice University, U.S.A.). This work was supported by Swiss National Foundation (Project 21-28467.90) and Sandoz S.A. (Fonds pour le Rhin).

REFERENCES

Ali W., O'Melia C. R. and Edzwald J. K. (1984) Colloidal stability of particles in lakes: measurement and significance. *Wat. Sci. Technol.* **17,** 701–712.

Baker J. E., Capel P. D. and Eisenreich S. J. (1986) Influence of colloids on sediment–water partition coefficients of polychlorophenyl congeners in natural waters. *Envir. Sci. Technol.* **20,** 1136–1143.

Beckett R., Nicholson G., Hart B. T., Hansen M. and Giddings J. C. (1988) Separation and size characterization of colloidal particles in river water by sedimentation field-flow fractionation. *Wat. Res.* **22,** 1535–1545.

Birkner F. B. and Morgan J. J. (1968) Polymer flocculation kinetics of dilute colloidal suspensions. *J. Am. Wat. Wks Ass.* **60,** 175–191.

Bott S. E. (1988) Enhanced resolution particle size distributions by multi-angle photon correlation spectroscopy. In *Particle Size Analysis 1988* (Edited by Lloyd P. J.), pp. 77–89. Wiley, New York.

Buffle J. (1988) *Complexation Reactions in Aquatic Systems: An Analytical Approach.* Horwood, Chichester.

Comba M. E. and Kaiser K. L. E. (1990) Suspended particulate concentrations in the St. Lawrence River (1985–1987) determined by centrifugation and filtration. *Sci. Total Envir.* **97/98,** 191–206.

CRC Handbook of Chemistry and Physics, 70th edition (1989) CRC Press, Boca Raton, Fla.

Edzwald J. K., Upchurch J. B. and O'Melia C. R. (1974) Coagulation in estuaries. *Envir. Sci. Technol.* **8,** 58–63.

Filella M. and Buffle J. (1993) Factors controlling the stability of submicron colloids in natural waters. *Colloids Surf.* **73,** 255–273.

Filella M., Buffle J. and Leppard G. G. (1993) Characterization of submicron colloids in freshwaters: evidence for their bridging by organic structures. *Wat. Sci. Technol.* **27,** 91–102.

Ford N. C. (1983) The theory and practice of correlation spectroscopy. In *Measurement of Suspended Particles by Quasi-elastic Light Scattering* (Edited by Danke B. E.), pp. 31–77. Wiley, New York.

Ford T. E. and Lock M. A. (1985) A temporal study of colloidal and dissolved organic carbon in rivers: apparent molecular weight spectra and their relationship to bacterial activity. *Oikos* **45,** 71–78.

Friedlander S. K. (1960) On the particle size spectrum of atmospheric aerosols. *J. Metereol.* **17,** 373–374.

Friedlander S. K. (1977) *Smoke, Dust and Haze.* Wiley–Interscience, New York.

Gallegos C. L. and Menzel R. G. (1987) Submicron size distributions of inorganic suspended solids in turbid waters by Photon Correlation Spectroscopy. *Wat. Resour. Res.* **23,** 596–602.

Gibbs R. J. (1983) Effect of natural organic coatings on the coagulation of particles. *Envir. Sci. Technol.* **17,** 237–240.

Hahn H. H. and Stumm W. (1968) Kinetics of coagulation with hydrolyzed Al(III). *J. Colloid Interface Sci.* **28,** 134–144.

Hiraide M., Ueda T. and Mizuike A. (1989) Humic and other negatively charged colloids of iron and copper in river water. *Analyt. chim. Acta* **227,** 421–424.

Hirtzel C. S. and Rajagopalan R. (1985) *Colloidal Phenomena. Advanced Topics.* Noyes, Park Ridge.

Hoffmann M. R., Yost E. C., Eisenreich S. J. and Maier W. J. (1981) Characterization of soluble and colloidal-phase metal complexes in river water by ultrafiltration. A mass balance approach. *Envir. Sci. Technol.* **15,** 655–661.

Jerlov N. G. (1976) *Marine Optics.* Elsevier, New York.

Karaiskakis G., Graff K. A., Caldwell K. D. and Giddings J. C. (1982) Sedimentation field-flow fractionation of colloidal particles in river waters. *Int. J. envir. analyt. Chem.* **12,** 1–15.

Kebler D. G., Bales R. C. and Amy G. L. (1989) Coagulation of submicron colloids by supramicron silica particles. *Wat. Sci. Technol.* **21,** 519–528.

Lawler D. F., O'Melia C. R. and Tobiason J. E. (1980) Integral water treatment plant design: from particle size to plant performance. In *Particulates in Water. Characterization, Fate, Effects, and Removal* (Edited by Kavanaugh M. C. and Leckie J. O.), pp. 353–388. ACS, Washington, D.C.

Laxen D. P. H. and Chandler I. M. (1983) Size distribution of iron and manganese species in freshwaters. *Geochim. cosmochim. Acta* **47,** 731–741.

Leenheer J. A., Meade R. H., Taylor H. E. and Pereira W. E. (1988) Sampling, fractionation, and dewatering of suspended sediment from the Mississippi River for geochemical and trace-contaminant analysis. USGS Water-Resources Investigations Report 88-4220, pp. 501–511.

Lerman A. (1979) *Geochemical Processes.* Wiley–Interscience, New York.

Lerman A., Carder K. L. and Betzer P. R. (1977) Elimination of fine suspensoids in the oceanic water column. *Eth Planet. Sci. Lett.* **37,** 61–70.

Lock M. A. and Ford T. E. (1986) Colloidal and dissolved organic carbon dynamics in undisturbed boreal forest catchments: a seasonal study of apparent molecular weight spectra. *Freshwat. Biol.* **16,** 187–195.

McCave I. N. (1984) Size spectra and aggregation of suspended particles in the deep ocean. *Deep-Sea Res.* **31,** 329–352.

Morel F. M. M. and Gschwend P. M. (1987) The role of colloids in the partitioning of solutes in natural waters. In *Aquatic Surface Chemistry. Chemical Processes at the Particle–Water Interface* (Edited by Stumm W.), pp. 405–422. Wiley–Interscience, New York.

Newman M. E. and Buffle J. (1994) Capabilities of photon correlation spectroscopy for determining size distributions of submicron colloids in natural waters. In preparation.

Nomizu T., Goto K. and Mizuike A. (1988) Electron microscopy of nanometer particles in freshwater. *Analyt Chem.* **60,** 2653–2656.

Nomizu T., Nozue T. and Mizuike A. (1987) Electron microscopy of submicron particles in natural waters—morphology and elemental analysis of particles in fresh waters. *Mikrochim. Acta* **2,** 99–106.

O'Melia C. R. (1980) Aquasols: the behavior of small particles in aquatic systems. *Envir. Sci. Technol.* **14,** 1052–1060.

O'Melia C. R. (1987) Particle–particle interactions. In *Aquatic Surface Chemistry. Chemical Processes at the Particle–Water Interface* (Edited by Stumm W.), pp. 385–403. Wiley–Interscience, New York.

O'Melia C. R. and Bowman K. S. (1984) Origins and effects of coagulation in lakes. *Schweiz. Z. Hydrol.* **46,** 64–85.

O'Melia C. R., Wiesner M., Weilenmann U. and Ali W. (1985) The influence of coagulation and sedimentation on the fate of particles, associated pollutants, and nutrients in lakes. In *Chemical Processes in Lakes* (Edited by Stumm W.), pp. 207–224. Wiley–Interscience, New York.

Orlandini K. A., Penrose W. R., Harvey B. R., Lovett M. B. and Findlay M. W. (1990) Colloidal behavior of actinides in an oligotrophic lake. *Envir. Sci. Technol.* **24,** 706–712.

Perret D., Newman M. E., Nègre J.-C., Chen Y. and Buffle J. (1994) Submicron particles in the Rhine River—I. Physico-chemical characterization. *Wat. Res.* **28,** 91–106.

Pizarro J., Belzile N., Filella M., Leppard G. G., Perret D. and Buffle J. (1994) Factors affecting coagulation/sedimentation of lake-born iron oxyhydroxide particles. Submitted to *Wat. Res.*

Rees T. F. (1990) Comparison of photon correlation spectroscopy with photosedimentation analysis for the determination of aqueous colloid size distributions. *Wat. Resour. Res.* **26,** 2777–2781.

Rees T. F. and Ranville J. F. (1990) Collection and analysis of colloidal particles transported in the Mississippi River, USA. *J. Contam. Hydrol.* **6,** 241–250.

Salbu B. and Bjørnstad H. E. (1990) Analytical techniques for determining radionuclides associated with colloids in waters. *J. Radioanalyt. Nucl. Chem.* **138,** 337–346.

Salbu B., Bjørnstad H. E., Lydersen E. and Pappas A. C. (1987) Determination of radionuclides associated with colloids in natural waters. *J. Radioanalyt. Nucl. Chem.* **115,** 113–123.

Schurtenberger P. and Newman M. E. (1993) Characterization of biological and environmental particles using static and dynamic light scattering. In *Environmental Particles: II* (Edited by van Leeuwen H. P. and Buffle J.). Lewis Publishers, Chelsea, Mich.

Sigleo A. C. and Means J. C. (1990) Organic and inorganic components in estuarine colloids: Implications for sorption and transport of pollutants. *Rev. envir. contam. Toxicol.* **112,** 123–147.

Stumm W. (1977) Chemical Interaction in partical separation. *Envir. Sci. Technol.* **11,** 1066–1070.

Stumm W. and Morgan J. J. (1981) *Aquatic Chemistry. An Introduction Emphasizing Chemical Equilibria in Natural Waters*, pp. 647–674. Wiley–Interscience, New York.

Swift D. L. and Friedlander S. K. (1964) The coagulation of hydrosols by Brownian motion and laminar shear flow. *J. Colloid Sci.* **19,** 621–647.

Tipping E. and Higgins D. C. (1982) The effect of adsorbed humic substances on the colloid stability of haematite particles. *Colloids Surf.* **5,** 85–92.

Van de Meent D., Los A., Leeuw J. W., Schenck P. A. and Haverkamp J. (1983) Size fractionation and analytical pyrolysis of suspended particles from the River Rhine delta. In *Adv. Organ. Geochem. 1981* (Edited by Bjorøy M. *et al.*), pp. 336–349. Wiley, Chichester.

Van der Meeren P. P. A., Vanderdeelen J. and Baert L. (1988) Optimization of quasi-elastic light scattering measurements. In *Particle Size Analysis 1988* (Edited by Lloyd P. J.), pp. 101–107. Wiley, New York.

Von Smoluchowski M. (1918) Versuch einer mathematischen Theorie der Koagulationskinetik kolloider Lösungen. *Z. Physik. Chem. (Leipzig)* **92,** 129–168.

Waber U. E., Lienert C. and Von Gunten H. R. (1990) Colloid-related infiltration of trace metals from a river to shallow groundwater. *J. Contam. Hydrol.* **6,** 251–265.

Weilenmann U., O'Melia C. R. and Stumm W. (1989) Particle transport in lakes: models and measurements. *Limnol. Oceanogr.* **34,** 1–18.

Zumstein J. and Buffle J. (1989) Circulation of pedogenic and aquagenic organic matter in an eutrophic lake. *Wat. Res.* **23,** 229–239.